

# Corrosion Behavior of Deep Water Oil Production Tubing Material Under Supercritical CO<sub>2</sub> Environment: Part 2—Effect of Crude Oil and Flow

F. Farelas,\* Y.S. Choi,<sup>†</sup>\* S. Nešić,\* Alvaro Augusto O. Magalhães,\*\* and Cynthia de Azevedo Andrade\*\*

## ABSTRACT

Deep water oil production tubing materials are exposed to high carbon dioxide (CO<sub>2</sub>) pressure and temperature conditions that can affect the corrosion performance of such materials. The present study evaluated the corrosion behavior of carbon steel exposed to supercritical CO<sub>2</sub>/oil/brine mixtures at different water cuts (0, 30, 50, 70, and 100%), CO<sub>2</sub> partial pressures (8 MPa and 12 MPa), and temperatures (65°C and 90°C) in a flowing 25 wt% sodium chloride (NaCl) solution. Corrosion behavior of carbon steel was evaluated by using electrical resistance (ER) measurements, weight-loss measurements, and surface analytical techniques (scanning electron microscopy [SEM] and energy-dispersive x-ray spectroscopy [EDS]). The corrosion rates of carbon steel increased with increasing water cut. There was no indication of corrosion attack with 0% water cut. At lower water cuts (30% and 50%), the steel surface was covered by iron carbonate (FeCO<sub>3</sub>), while iron carbide (Fe<sub>3</sub>C) was present on the steel surface at higher water cuts (70% and 100%) with very high corrosion rates. In addition, the presence of flow prevented the formation of protective FeCO<sub>3</sub> at high water cut conditions.

**KEY WORDS:** carbon steel, CO<sub>2</sub> corrosion, crude oil, FeCO<sub>3</sub>, supercritical CO<sub>2</sub>, water cut

Submitted for publication: May 9, 2013. Revised and accepted: August 1, 2013. Preprint available online: August 8, 2013. doi: <http://dx.doi.org/10.5006/1020>. Part 1 appeared in *CORROSION* 70, 1 (2014), p. 38-47.

<sup>†</sup> Corresponding author. E-mail: [choiy@ohio.edu](mailto:choiy@ohio.edu).

\* Institute for Corrosion and Multiphase Technology, Department of Chemical and Biomolecular Engineering, Ohio University, Athens, OH 45701.

\*\* Petrobras Rio de Janeiro, RJ 21941-915 Brazil.

<sup>(1)</sup> American Petroleum Institute (API), 1220 L St. NW, Washington, DC 20005.

## INTRODUCTION

Deep water oil production tubing materials usually are exposed to high carbon dioxide (CO<sub>2</sub>) pressure and temperature conditions that can affect the corrosion performance of such materials. At temperatures above 31.1°C and pressures higher than 7.38 MPa, CO<sub>2</sub> is in its supercritical state. In the absence of water, supercritical CO<sub>2</sub> is not corrosive; however, under normal oil production operations, produced water is always present. When CO<sub>2</sub> dissolves in water, carbonic acid (H<sub>2</sub>CO<sub>3</sub>) is formed, which significantly increases the corrosion rate of carbon steels. The mechanisms of CO<sub>2</sub> corrosion under supercritical conditions do not change compared to those identified at lower partial pressure.<sup>1</sup> An increase in the CO<sub>2</sub> partial pressure usually results in a drastic increase in the corrosion rate behavior that is enhanced with temperature and flow.<sup>2-3</sup>

In corrosion, along with the behavior of deep water, oil production tubing materials, and the general factors (CO<sub>2</sub> partial pressure, temperature, and flow), another important parameter has to be taken into account: the presence of crude oil. Carew, et al.,<sup>4</sup> studied the effect of water cut, CO<sub>2</sub>, and hydrogen sulfide (H<sub>2</sub>S) partial pressures, temperature, and flow velocity on the corrosion rate of API 5CT<sup>(1)</sup> L80 steel. A mixture of 80% CO<sub>2</sub>:20% H<sub>2</sub>S was injected to the system and the pressure was increased up to ~20 MPa with nitrogen. The corrosion increased with water cut and no significant corrosion attack occurred at water cuts between 30% and 40%; however, general and local-

**TABLE 1**  
Test Matrix for Corrosion Testing

CO <sub>2</sub> Pressure (MPa)	CO <sub>2</sub> Phase	Temperature (°C)	Water Cut (%)	Rotation Speed (rpm)	Time (h)	Measurement Techniques	Surface Analysis
8 12	Supercritical	90 65	0, 30, 50, 70, 100	1,000	48	ER and weight loss	SEM, EDS, IFM

**TABLE 2**  
Element Analysis by Atomic Emission Spectroscopy for the Carbon Steel (API 5CT L80) (wt%)

C	Cr	Mn	P	S	Si	Fe
0.30	0.85	0.91	0.015	0.008	0.29	Balance

ized attack was observed at water cuts greater than 40%. It was also reported that an increase in the rotational speed from 1,000 rpm to 4,000 rpm did not have a significant effect on the corrosion rate.<sup>4-5</sup> The effect of supercritical CO<sub>2</sub> in multiphase flow using different pipeline steels has also been investigated.<sup>6</sup> It was reported that the corrosion rate increased with the water cut, and below 50% water cut, the mixture was in the water-in-oil state. However, at water cuts greater than 50%, the mixture switched to oil-in-water resulting in high general corrosion rate and pitting corrosion. Although studies on the general aqueous CO<sub>2</sub> corrosion in oil/water mixtures have been carried out and reported, there are no comprehensive studies available for crude oil/CO<sub>2</sub>/brine environments at supercritical CO<sub>2</sub> conditions.

The overall objective of the study was to evaluate the corrosion behavior of carbon steel in crude oil/supercritical CO<sub>2</sub>/brine mixtures related to the deep water oil production development. In Part 1 of this study,<sup>7</sup> the corrosion properties of carbon steel were evaluated under different CO<sub>2</sub> partial pressures (4, 8, and 12 MPa) and temperatures (65 and 90°C) in a 25 wt% NaCl aqueous solution. In Part 2 of the same study, the goal was to evaluate the corrosion behavior of carbon steel exposed to crude oil/supercritical CO<sub>2</sub>/brine mixtures at different water cuts (0, 30, 50, 70, and 100%) in a flowing 25 wt% NaCl solution.

## EXPERIMENTAL PROCEDURES

Corrosion experiments were carried out in a 4 L stainless steel autoclave. Details of the experimental setup are given in Part 1 of this study.<sup>7</sup> 28 API crude oil was used in these experiments and water cut was varied from 0 to 100% with a 25 wt% NaCl solution.

Table 1 shows the test matrix for corrosion testing. The experimental parameters were chosen based on the results obtained in Part 1 of this study,<sup>7</sup> where localized corrosion was observed.

Depending on the water cut selected for the test (Table 1), crude oil and 25 wt% NaCl aqueous solution

were placed together in a beaker and stirred overnight to form an emulsion. Then, the emulsion was transferred to the autoclave and deoxygenated with CO<sub>2</sub> for 1 h to 3 h. Meanwhile, two square-type API 5CT L80 carbon steel samples (1.27 cm by 1.27 cm by 0.254 cm), with the chemical composition shown in Table 2, were ground with 600-grit silicon carbide (SiC) paper, cleaned with isopropyl alcohol (C<sub>3</sub>H<sub>8</sub>O) in an ultrasonic bath, and dried. Subsequently, an electrical resistance (ER) probe and the steel specimens were placed into the autoclave.

The ER probe element was machined from the same material as the weight-loss samples. The element is a wire loop with 2.03 mm thickness and a useful life of 0.5 mm. In ER measurement, the reduction in the cross-sectional area of an element of metal as it corrodes is accompanied by a corresponding increase in the electrical resistance (R) of the element. The relationship is given by Equation (1):<sup>8</sup>

$$R = r \times \frac{L}{A} \quad (1)$$

where L is the carbon steel element length, A is the cross-sectional area, and r is the specific resistance. The probe reading represents the percentage of the effective probe element thickness consumed since the probe was inserted into the corrosive system. This value is most commonly used to calculate metal loss and/or corrosion rate, as shown in Equations (2) and (3):<sup>8</sup>

$$ML = \frac{X \times K}{1,000} \quad (2)$$

$$CR = \frac{(X_2 - X_1) \times K \times 365}{1,000 \times T} \quad (3)$$

where ML is metal loss in mils, X is the instrument reading at any given time, K is the probe constant (= 20), X<sub>2</sub> is the instrument reading at time T<sub>2</sub>, X<sub>1</sub> is the instrument reading at time T<sub>1</sub>, T is time lapse (days) between readings X<sub>1</sub> and X<sub>2</sub>, and CR is the corrosion rate (mpy).

After closing the autoclave, an impeller was used to stir the emulsion at a rotation speed of 1,000 rpm; stirring was maintained during the test (48 h). Temperature was increased to the testing temperature and high-pressure CO<sub>2</sub> was injected with a booster pump.

After each test, the specimens were removed from the autoclave, rinsed with toluene, acetone, deionized water and isopropyl alcohol, dried with  $N_2$ , and stored in a desiccator cabinet for surface analysis by scanning electron microscopy (SEM) and energy-dispersive x-ray spectroscopy (EDS).

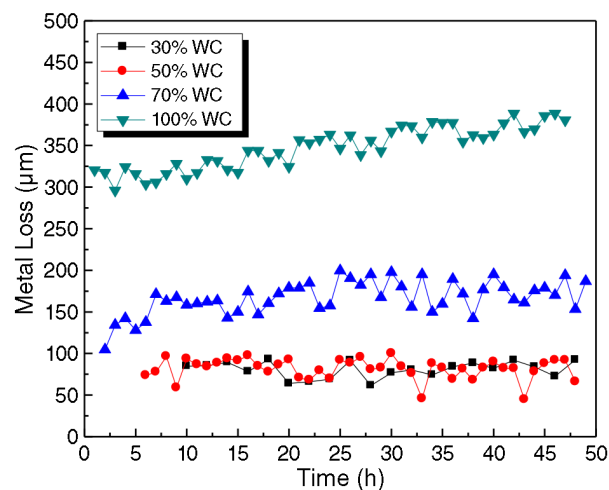
## RESULTS AND DISCUSSION

### Experimental Study of Corrosion in $CO_2$ /Oil/Water Environments

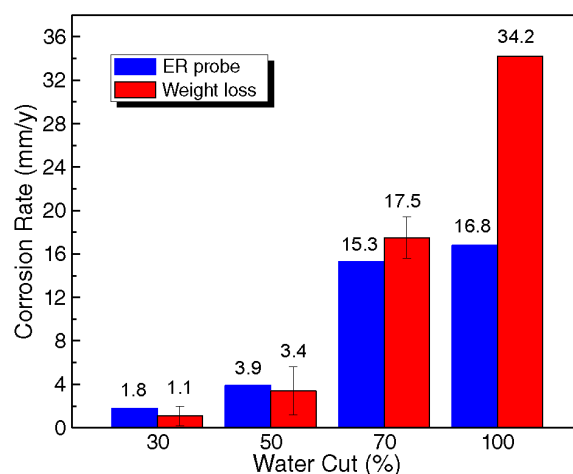
**Experiments at 8 MPa and 90°C** — Figure 1 shows the variation of metal loss with time obtained from ER measurements with different water cuts at 8 MPa and 90°C. The water cut was varied from 30% to 100%. The metal loss with 30% and 50% water cuts were quite similar and constant during the 48 h of exposure. With 70% water cut, the initial metal loss was higher than that seen at lower water cut cases and slightly increased with time. Without the oil phase (100% water cut), the initial metal loss was much higher compared to lower water cuts and kept increasing during the 48 h of exposure.

Figure 2 compares the average corrosion rate obtained from ER and weight-loss measurements under different water cuts. As can be observed from Figure 2, the corrosion rate increased considerably with the increase of water cut. The corrosion rate slightly increased by increasing the water cut from 30% to 50%, whereas it increased more than four times from 50% to 70% water cut. It can be assumed that the oil and water mixture was in its water-in-oil state below 50% of the water cut, whereas the mixture was changed to the oil-in-water state at higher water cuts.<sup>6</sup> However, it is important to note that even at low water cuts (30% and 50%), the corrosion rate was not negligible (e.g., 1.1 mm/y at 30% water cut and 3.4 mm/y at 50% water cut). Figure 2 also shows that the corrosion rates from both ER and weight-loss measurements showed the same trend with different water cuts. However, there is a significant difference in corrosion rate between ER and weight-loss measurements at 100% water cut, and it can be attributed to the presence of conductive layers that can affect the ER measurements.<sup>9</sup> In Part 1 of this study,<sup>7</sup> the presence of iron carbide ( $Fe_3C$ ) on the steel surface was detected using XRD analysis. Farelas, et al.,<sup>10</sup> and Berntsen, et al.,<sup>11</sup> reported as well the presence of a  $Fe_3C$  layer resulting from the preferential dissolution of ferrite over  $Fe_3C$ .  $Fe_3C$  is an electrical conductor<sup>12</sup> and its presence will increase the apparent cross-sectional area of the ER element and decrease the element's electrical resistance (Equation [1]), which results in lowering the corrosion rate reading, as is observed in Figure 2.

SEM surface observations and EDS analyses of the samples exposed to different water cuts are shown in Figure 3. Note that the morphologies were



**FIGURE 1.** Variation of metal loss with time obtained from ER measurements at different water cuts (8 MPa  $CO_2$ , 90°C, 1,000 rpm).



**FIGURE 2.** Comparison of corrosion rates obtained from ER and weight-loss measurements (average) with different water cuts at 48 h (8 MPa  $CO_2$ , 90°C, 1,000 rpm).

almost identical for 30% and 50% water cuts, and the EDS analysis of the surface suggested that it was covered predominantly by  $FeCO_3$  (Figures 3[a] and [b]).

For 70% and 100% water cut conditions, the steel surface appears to be in a much more severely attacked state. EDS analysis suggested that the corrosion product consists mainly of  $Fe_3C$  with minor constituents of alloying elements from carbon steel. Although some  $FeCO_3$  was found on the surface at 70% water cut, as illustrated in Figure 3(c), it did not offer any protection against corrosion under this particular condition.

Figure 4 shows the surface morphologies of samples after removing the corrosion product layer with Clarke's solution.<sup>13</sup> At 30% and 50% water cut conditions, the original polishing marks were still visible on a fraction of the surface, suggesting that it did not

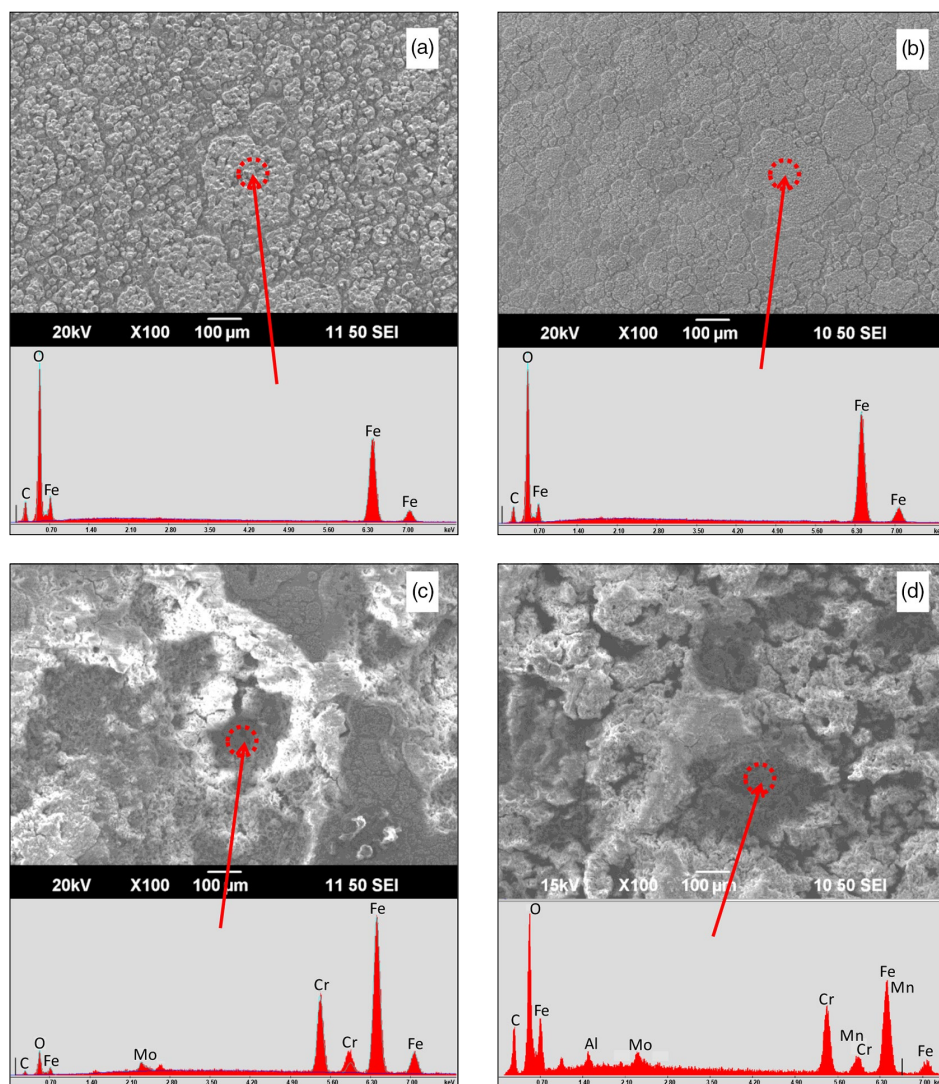


**FIGURE 3.** SEM images and EDS spectra of the corroded surface of the sample exposed to: (a) 30%, (b) 50%, (c) 70%, and (d) 100% water cut (8 MPa, 90°C, 48 h, 1,000 rpm).

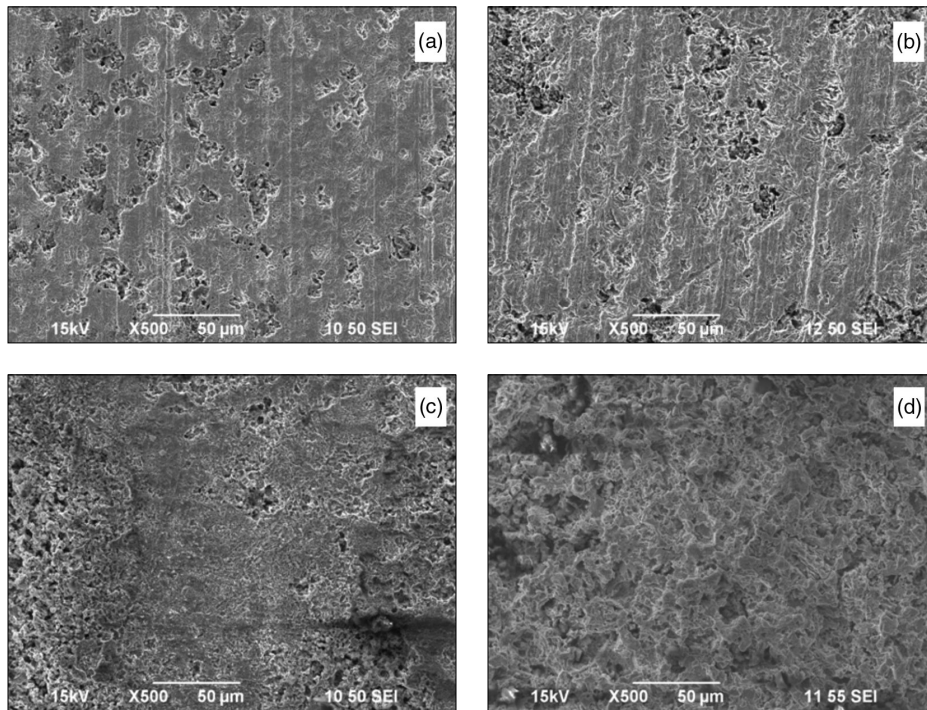
corrode much. A non-uniform corrosion attack can be observed at 30% and 50% water cut conditions. On the other hand, a severe uniform corrosion attack was observed on the surface for samples at 70% and 100% water cut conditions.

**Experiments at 12 MPa and 65°C** — Figure 5 shows the variation of metal loss with time obtained from ER measurements with different water cuts at 12 MPa and 65°C. Figure 6 compares the average corrosion rate obtained from ER, linear polarization resistance (LPR), and weight-loss measurements at different water cuts. Similar to the results obtained at 8 MPa and 90°C, the corrosion rate increased with the increase in water cut. For 30% and 50% water cut conditions, the average corrosion rate was relatively lower than that of 70% and 100% conditions, but the corrosion rate was not negligible (e.g., 1.5 mm/y at 30% water cut and 6.0 mm/y at 50% water cut). No significant metal loss was observed by ER and weight-

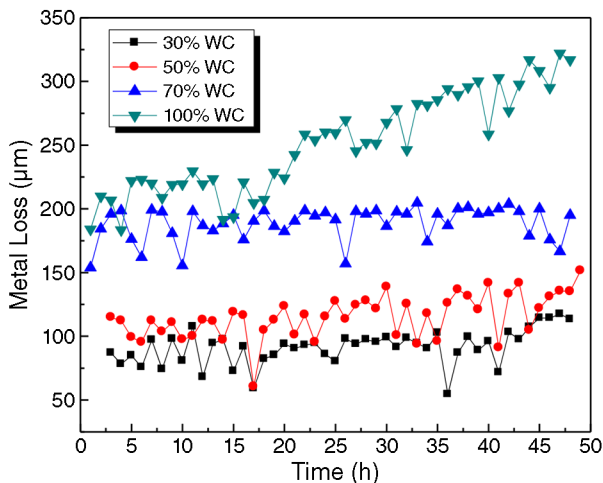
loss measurements for the condition without water (0% water cut).

Figure 6 also shows that the corrosion rates obtained from ER, weight-loss, and LPR measurements all indicated very high values at 100% water cut. The difference between weight-loss and LPR measurements could be attributed to the arbitrary B value (26 mV) used for calculating the corrosion rate in the electrochemical measurements.

The SEM surface observations of the samples exposed to different water cuts are shown in Figure 7. For 0% water cut condition, no visible signs of corrosion were observed on the sample, i.e., the surfaces appeared shiny and void of any type of corrosion products (Figure 7[a]). For 30% and 50% water cut, it can be seen that the surface morphologies were almost identically covered by  $\text{FeCO}_3$  (Figures 7[b] and [c]). For 70% and 100% water cut conditions, most of the surface was severely attacked and the corrosion



**FIGURE 4.** SEM images of the corroded surface of samples after cleaning: (a) 30%, (b) 50%, (c) 70%, and (d) 100% water cut (8 MPa, 90°C, 48 h, 1,000 rpm).



**FIGURE 5.** Variation of metal loss with time obtained from ER measurements at different water cuts (48 h, 12 MPa  $\text{CO}_2$ , 65°C, 1,000 rpm).

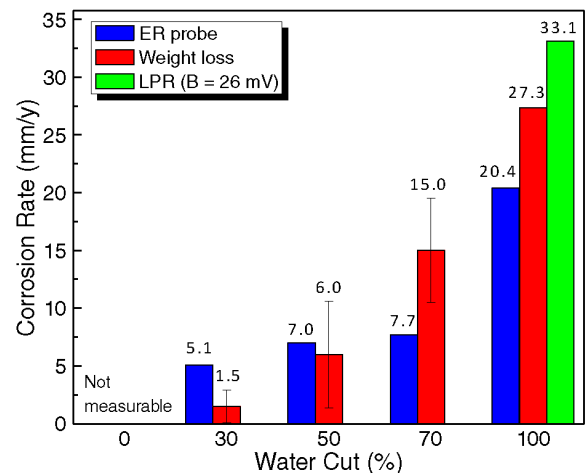


**FIGURE 6.** Comparison of corrosion rates obtained from ER and weight-loss measurements (average) with different water cuts (48 h, 12 MPa  $\text{CO}_2$ , 65°C, 1,000 rpm).

product consists mainly of  $\text{Fe}_3\text{C}$  and minor constituents of alloying elements from carbon steel (Figures 7[d] and [e]).

Figure 8 shows the surface morphologies of samples after removing the corrosion product layer with Clarke's solution. At 30% and 50% water cut conditions, the polishing marks were still visible on parts of the surface, with some scattered corrosion attack. At 70% and 100% water cut conditions, severe uniform corrosion attack was observed on the surface of the

samples. For 70% water cut condition, infinite force microscopy (IFM) analysis (Figure 9) revealed that the depth of the penetration was around 85.5  $\mu\text{m}$ , which corresponds to 15.6 mm/y. This penetration rate is similar to the weight-loss corrosion rate shown in Figure 6 (15 mm/y), confirming uniform attack.

**Corrosion Rate Comparison Between 8 MPa-90°C and 12 MPa-65°C Conditions** — Figure 10 compares the corrosion rate obtained from weight-loss measurements under different conditions as a function of

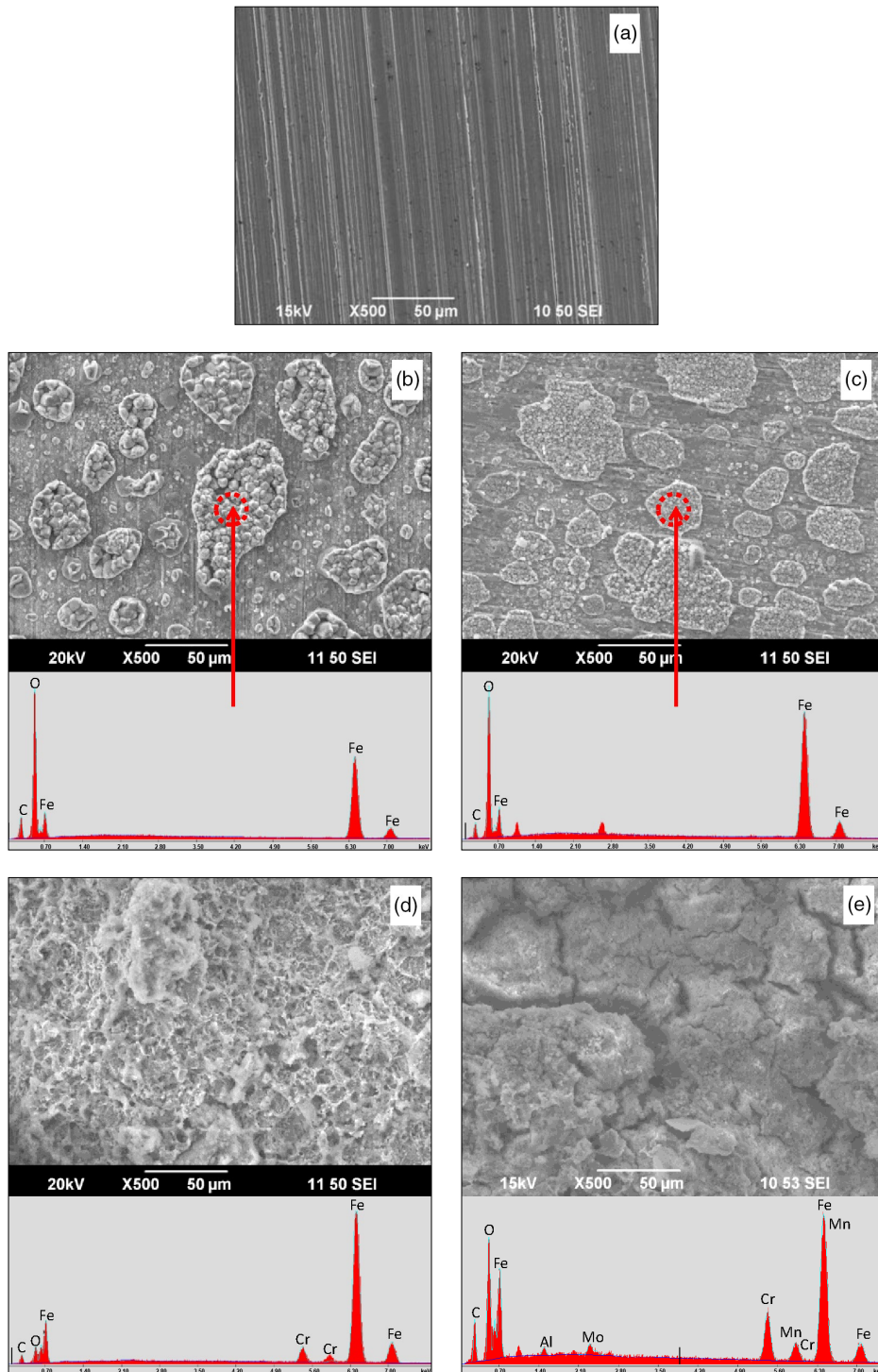


**FIGURE 7.** SEM images and EDS spectra of the corroded surface of the sample exposed to: (a) 0%, (b) 30%, (c) 50%, (d) 70%, and (e) 100% water cut (12 MPa, 65°C, 48 h, 1,000 rpm).

water cut. For both conditions, the corrosion rate increased with the increase of water cut. In the mixture of crude oil and water (30% ~ 70% water cut), there is no significant difference in corrosion rate between two conditions. However, it showed higher corrosion rate in the 8 MPa-90°C condition than 12 MPa-65°C, as a result of the higher temperature which accelerates the

corrosion process more than the partial pressure of CO<sub>2</sub> did.

#### *Effect of Flow on the Corrosion Behavior of Carbon Steel with 100% Water Cut*

It is well known that the presence of flow affects CO<sub>2</sub> corrosion rate since it can enhance the transport

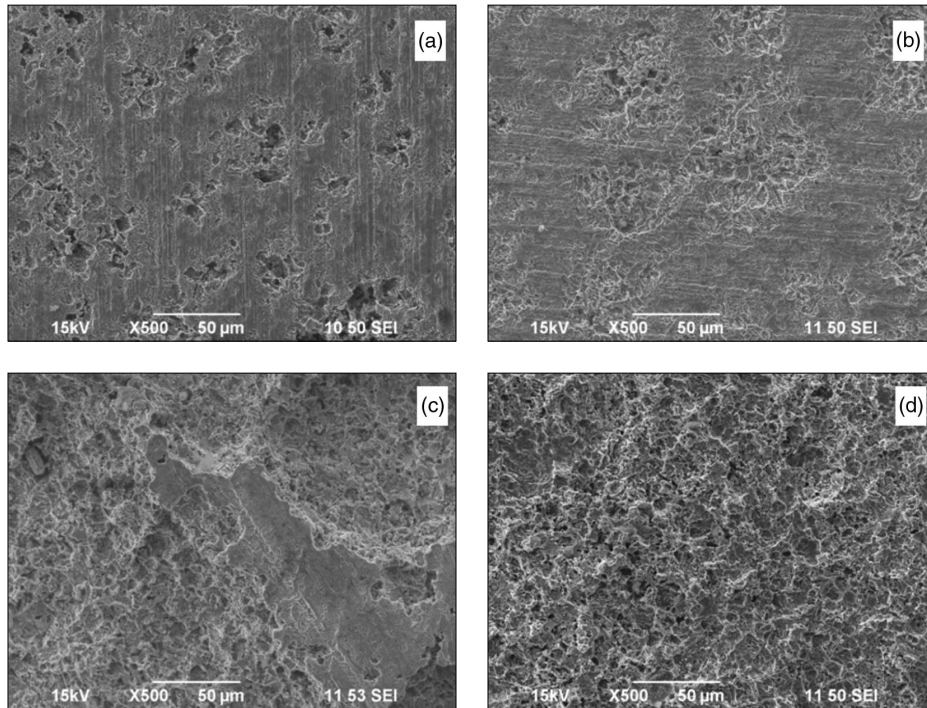


**FIGURE 8.** SEM images of the corroded surface of samples after cleaning: (a) 30%, (b) 50%, (c) 70%, and (d) 100% water cut (12 MPa, 65°C, 48 h, 1,000 rpm).

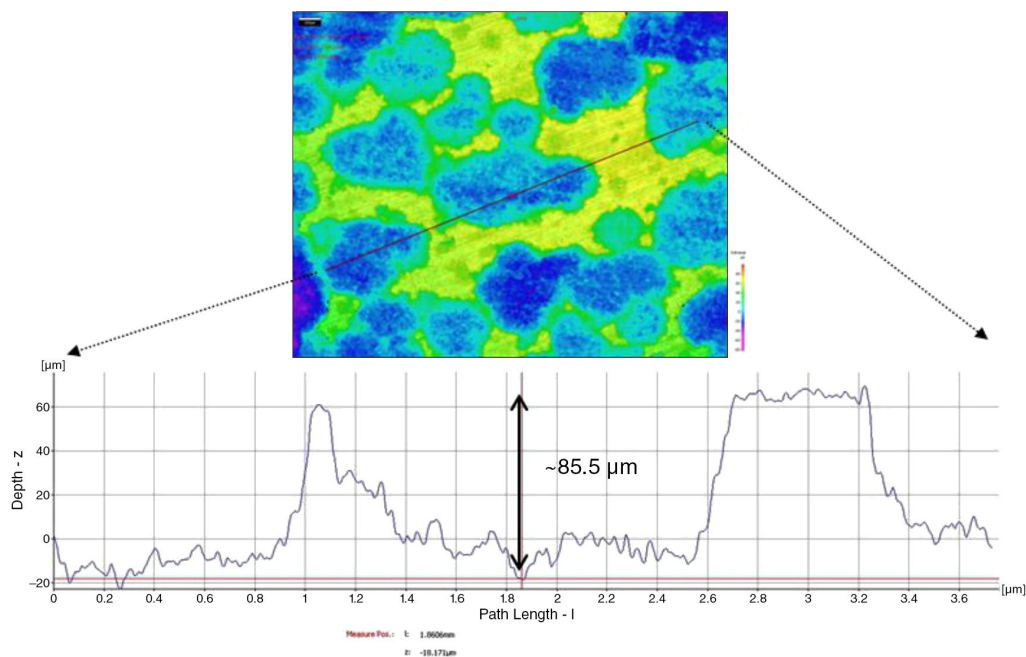


**FIGURE 9.** Surface profile analysis on cleaned surface of the sample exposed to 70% water cut condition at 12 MPa and 65°C for 48 h (1,000 rpm).

of corrosive species toward and away from the metal surface. In addition, when the flow rate is sufficiently high, it can prevent the formation of  $\text{FeCO}_3$ .<sup>14</sup>

Figure 11 compares the corrosion rate of carbon steel obtained from weight-loss measurements in a 25 wt% NaCl solution with and without flow. As men-

tioned in the “Experimental Procedures” section, fast stirring (i.e., 1,000 rpm) was achieved using a stainless steel impeller at the bottom of the autoclave. The corrosion rates for both conditions showed higher values than those without flow. In particular, the corrosion rate at 8 MPa-90°C condition increased from

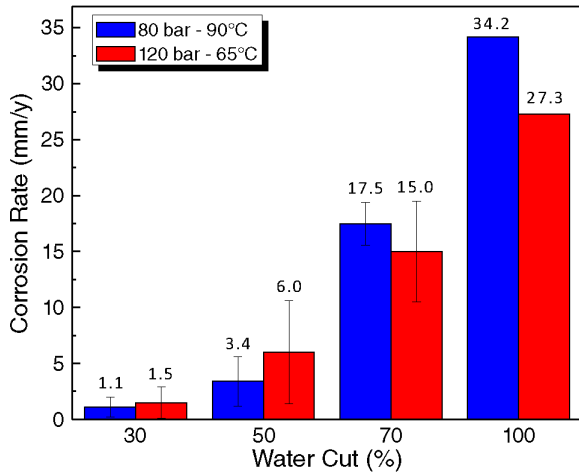


**FIGURE 10.** Comparison of corrosion rates obtained from weight-loss measurements with different testing conditions and water cuts.

5.6 mm/y (without flow) to 34.2 mm/y (with flow). It is important to mention that without flow the corrosion rate measured using LPR showed a corrosion rate of 0.05 mm/y after 112 h of exposure because of the presence of  $\text{FeCO}_3$ .<sup>7</sup>

Figure 12 shows the SEM surface images of the samples exposed to a 25 wt% NaCl solution at 8 MPa and 90°C with/without flow. Under stagnant condition, the surface was completely covered by protective  $\text{FeCO}_3$ , which somewhat decreased the corrosion rate with time (Figure 12[a]). However, there is no indication of the presence of protective  $\text{FeCO}_3$  on the surface under flowing conditions (Figure 12[b]), and it showed severe uniform corrosion. The difference in corrosion rates between stagnant and flowing conditions can be explained by the difference in water chemistry at the steel surface. Under stagnant conditions, a high con-

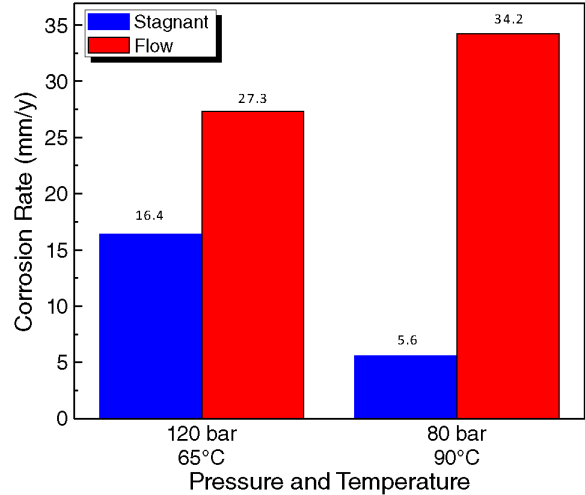


**FIGURE 11.** Effect of flow on the weight-loss corrosion rate of carbon steel exposed to a 25 wt% NaCl solution at different  $\text{CO}_2$  pressures and temperatures.

centration of ferrous ions ( $\text{Fe}^{2+}$ ) at the steel surface and the higher surface pH would have facilitated the formation of a protective  $\text{FeCO}_3$  layer, leading to lower corrosion rates. However, flow and associated enhanced mass transfer would have brought more corrosive species to the steel surface and could prevent the buildup of  $\text{Fe}^{2+}$  ions at the actively corroding steel surface, thereby preventing formation of a protective  $\text{FeCO}_3$  on the steel and leading to higher corrosion rates.

## CONCLUSIONS

❖ The corrosion rate of carbon steel increased with increasing water cut under the conditions used in this study (8 MPa-90°C and 12 MPa-65°C).

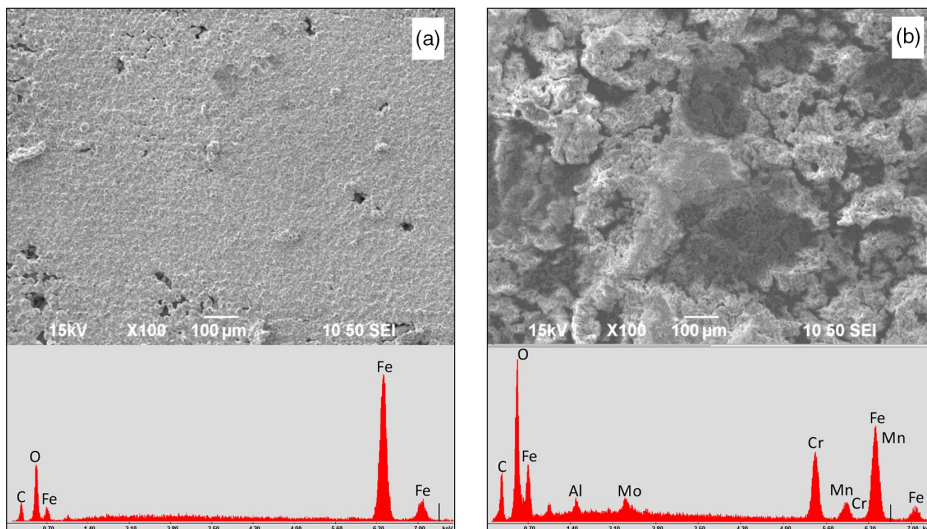


**FIGURE 12.** SEM images of the sample surfaces after being exposed to a 25 wt% NaCl solution at 8 MPa  $\text{CO}_2$  and 90°C for 48 h: (a) stagnant and (b) flowing (1,000 rpm).

- ❖ At low water cuts (30%, 50%), the sample surface was covered by some  $\text{FeCO}_3$ , whereas  $\text{Fe}_3\text{C}$  was predominantly present on the steel surface at higher water cuts (70%, 100%).
- ❖ Corrosion rates ranged from high (at 30% and 50% water cut) to catastrophic (at 70% and 100% water cut).
- ❖ Flow markedly enhanced the corrosion rate and hindered the formation of a protective  $\text{FeCO}_3$  layer when exposed to the aqueous phase (100% water cut). No localized corrosion was observed in the testing conditions.

#### REFERENCES

1. Y. Zhang, X. Pang, S. Qu, X. Li, K. Gao, *Corros. Sci.* 59 (2012): p. 186-197.
2. M.F. Suhor, M.F. Mohamed, A. Muhammad Nor, M. Singer, S. Nešić, "Corrosion of Mild Steel in High  $\text{CO}_2$  Environment: Effect of the  $\text{FeCO}_3$  Layer," CORROSION 2012, paper no. C2012-1434, (Houston, TX: NACE International, 2012).
3. A. Muhammad Nor, M.F. Suhor, M.F. Mohamed, M. Singer, S. Nešić, "Corrosion of Carbon Steel in High  $\text{CO}_2$  Containing Environments—The Effect of High Flow Rate," CORROSION 2012, paper no. C2012-1683 (Houston, TX: NACE, 2012).
4. J.A. Carew, A. Al-Sayegh, A. Al-Hashem, "The Effect of Water-Cut on the Corrosion Behaviour L80 Carbon Steel Under Downhole Conditions," CORROSION 2000, paper no. 61 (Houston, TX: NACE, 2000).
5. J. Carew, A. Al-Hashem, "CO<sub>2</sub> Corrosion of L-80 Steel in Simulated Oil Well Conditions," CORROSION 2002, paper no. 02299 (Houston, TX: NACE, 2002).
6. Z.D. Cui, S.L. Wu, C.F. Li, S.L. Zhu, X.J. Yang, *Mater. Lett.* 58 (2004): p. 1035-1040.
8. "Electrical Resistance E/R<sup>+</sup> Monitoring," available from: <http://www.alspi.com/erintro.htm>.
9. G.S. Frankel, *J. ASTM Int.* 5, 2 (2008), paper no. JAI101241.
7. Y.S. Choi, F. Farelas, S. Nešić, A.A.O. Magalhães, C. de Azevedo Andrade, *Corrosion* 70, 1 (2014): p. 38-47, <http://dx.doi.org/10.5006/1019>.
10. F. Farelas, B. Brown, S. Nešić, "Iron Carbide and Its Influence on the Formation of Protective Iron Carbonate in  $\text{CO}_2$  Corrosion of Mild Steel," CORROSION 2013, paper no. 2013-2291 (Houston, TX: NACE, 2013).
11. T. Berntsen, M. Seiersten, T. Hemmingsen, *Corrosion* 69 (2013): p. 601.
12. J. Crolet, N. Thevenot, S. Nešić, *Corrosion* 54 (1998): p. 194.
13. ASTM Standard G1-03, "Standard Practice for Preparing Cleaning and Evaluating Corrosion Test Specimens" (West Conshohocken, PA: ASTM International, 2003) .
14. S. Nešić, *Corros. Sci.* 49 (2007): p. 4308-4338.